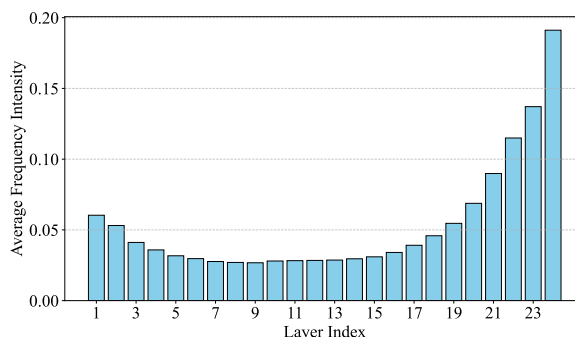


SpectralKD: A Unified Framework for Interpreting and Distilling Vision Transformers via Spectral Analysis

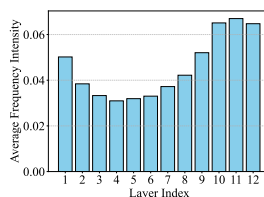
Huiyuan Tian¹ Bonan Xu² Shijian Li¹ Gang Pan¹

Abstract

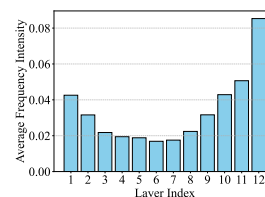
Knowledge Distillation (KD) has achieved widespread success in compressing large Vision Transformers (ViTs), but a unified theoretical framework for both ViTs and KD is still lacking. In this paper, we propose SpectralKD, a novel unified analytical framework that offers deeper insights into ViTs and optimizes KD via spectral analysis. Our model-wise analysis reveals that CaiT concentrates information in their first and last few layers, informing optimal layer selection for KD. Surprisingly, our layer-wise analysis discovers that Swin Transformer and CaiT exhibit similar spectral encoding patterns despite their architectural differences, leading to feature map alignment guideline. Building on these insights, we propose a simple yet effective spectral alignment method for KD. Benefiting from the deeper understanding by above analysis results, even such a simple strategy achieves state-of-the-art performance on ImageNet-1K without introducing any trainable parameters, improving DeiT-Tiny by +5.2% and Swin-Tiny by +1.4% in top-1 accuracy. Furthermore, our post-training analysis reveals that distilled students can reproduce spectral patterns similar to their teachers, opening a new area we term “distillation dynamics”. Code and experimental logs are available in <https://github.com/thy960112/SpectralKD>.



(a) CaiT-S24 (teacher).



(b) DeiT-T without distillation.



(c) DeiT-T by SpectralKD.

Figure 1. Model-wise frequency intensity analysis $L(\mathbf{X})$ (Equation 5), plotted across the Transformer depth for three models: (a) CaiT-S24 (teacher), (b) DeiT-Tiny without distillation, and (c) DeiT-Tiny distilled by our SpectralKD. SpectralKD clearly shifts the student’s intensities in different layers closer to those of the teacher, especially in the most information-rich layers in the early and final few layers. Both CaiT-S24 and baseline DeiT-Tiny checkpoints are taken from the *timm* library (Wightman, 2019).

1. Introduction

Benefiting from attention mechanisms, Transformer models (Vaswani, 2017) have achieved remarkable success across diverse applications (Devlin, 2018; Brown et al., 2020; Doso-

¹College of Computer Science and Technology, Zhejiang University, NO. 38 Zheda Road, Xihu District, Hangzhou 310027, China ²School of Aeronautics and Astronautics, Zhejiang University, NO. 38 Zheda Road, Xihu District, Hangzhou 310027, China. Correspondence to: Shijian Li <shijianli@zju.edu.cn>.

vitskiy, 2020; Han et al., 2021; Liu et al., 2021; Han et al., 2022; Xu et al., 2024; Li et al., 2024; Bar-Shalom et al., 2024). However, their substantial computational cost remains a significant challenge. KD (Hinton, 2015), an effective model compression technique, can accelerate inference and reduce resource requirements (Choudhary et al., 2020; Pham et al., 2024; Rao et al., 2024). To develop trustworthy and efficient models, it is crucial to gain deeper insights into both the internal encoding patterns of Transformer models and the mechanisms underlying KD.

Recently, researchers have made significant efforts (Abnar

& Zuidema, 2020; Raghu et al., 2021; Chefer et al., 2021; Yeh et al., 2023; Zimmermann et al., 2024; Zeng et al., 2024) to gain deeper insights into the attention mechanisms. Better interpretability (Pan et al., 2021; Caron et al., 2021; Yu & Xiang, 2023) can be leveraged to improve the efficiency of ViTs. Meanwhile, numerous theoretical analyses (Phuong & Lampert, 2019; Menon et al., 2021; Chandrasegaran et al., 2022; Allen-Zhu & Li, 2023) have also been conducted to reveal the internal mechanisms of KD. However, a unified theoretical framework that encompasses both ViTs and KD remains an open research challenge.

In this paper, we propose SpectralKD, a novel unified analytical framework that enhances our understanding of ViTs and optimizes the KD process via spectral analysis. Our key contributions are summarized as follows:

- **Model-wise analysis.** By analyzing intermediate feature maps in the frequency domain, our spectral analysis unveils a characteristic U-shaped frequency pattern in CaiT layers: early and late few layers capture richer spectral information, whereas middle layers encode lower-intensity frequencies. This model-wise observation provides guidelines for layer selection in KD when dealing with uniform Transformers.
- **Layer-wise insight.** Surprisingly, both hierarchical (Swin) and uniform (CaiT) transformer architectures exhibit similar encoding patterns, offering a potential explanation for strong generalization capabilities of ViTs. This layer-wise finding also suggests practical strategies for feature alignment in KD.
- **A simple, parameter-free KD strategy.** Building on the above insights, we propose a straightforward, parameter-free KD approach. Despite its simplicity, our method benefits from the interpretability provided by spectral analysis and achieves state-of-the-art (SOTA) performance.
- **Distillation dynamics.** Post-training analysis demonstrates that SpectralKD induces global changes in the student’s spectral patterns, even in layers not explicitly aligned. This result opens up a new area we term “distillation dynamics”, thus paving the way for more transparent and interpretable KD.

2. Spectral Analysis

In this section, we introduce SpectralKD, a unified analytical framework for ViTs and KD. Our framework provides quantitative insights into the information flow across network layers and unveils the underlying encoding patterns of ViTs. Unlike prior approaches relying primarily on empirical observations, SpectralKD offers a more theoretically grounded method to analyze and distill ViTs.

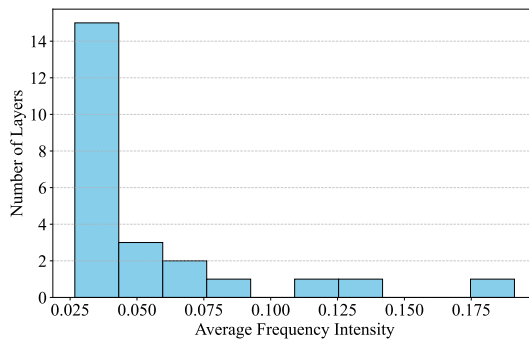


Figure 2. Histogram of the model-wise frequency intensities $L(\mathbf{X})$ (Equation 5) for all 24 layers of CaiT-S24. The distribution is heavily skewed: most layers have relatively low spectral intensity, while only a small number exhibit substantially higher values. These *peaks* point to potentially critical layers for knowledge distillation.

2.1. Analysis Method

Consider a batch of intermediate feature maps $\mathbf{X} \in \mathbb{R}^{B \times C \times H \times W}$ from a particular layer, where B is the batch size, C is the number of channels, and H and W denote the spatial height and width, respectively. We apply a one-dimensional Fast Fourier Transform (FFT) along the channel dimension to map these real-valued feature maps into the complex domain \mathbb{C} . Formally,

$$\mathcal{F}(\mathbf{X}) = \text{FFT}(\mathbf{X}), \quad (1)$$

where FFT indicates the 1D FFT applied independently for each spatial location (b, h, w) . This operation involves performing $B \times H \times W$ separate 1D FFTs over vectors of length C .

After obtaining the frequency domain representation $\mathcal{F}(\mathbf{X}) \in \mathbb{C}^{B \times C \times H \times W}$ of the feature maps, we compute the magnitude of each complex entry as follows:

$$\mathbf{A}(\mathbf{X}) = \sqrt{\text{Re}^2(\mathcal{F}(\mathbf{X})) + \text{Im}^2(\mathcal{F}(\mathbf{X}))}, \quad (2)$$

where $\text{Re}(\mathcal{F}(\mathbf{X}))$ and $\text{Im}(\mathcal{F}(\mathbf{X}))$ represent the real and imaginary components of $\mathcal{F}(\mathbf{X})$, respectively. This yields a real-valued tensor $\mathbf{A}(\mathbf{X}) \in \mathbb{R}^{B \times C \times H \times W}$.

Next, we average $\mathbf{A}(\mathbf{X})$ over the batch dimension B and spatial dimensions H and W :

$$\mathbf{S}(\mathbf{X}) = \frac{1}{B \times H \times W} \sum_{b=1}^B \sum_{h=1}^H \sum_{w=1}^W \mathbf{A}(\mathbf{X}). \quad (3)$$

obtaining $\mathbf{S}(\mathbf{X}) \in \mathbb{R}^C$. Each element of $\mathbf{S}(\mathbf{X})$ corresponds to the average spectral intensity of a particular frequency

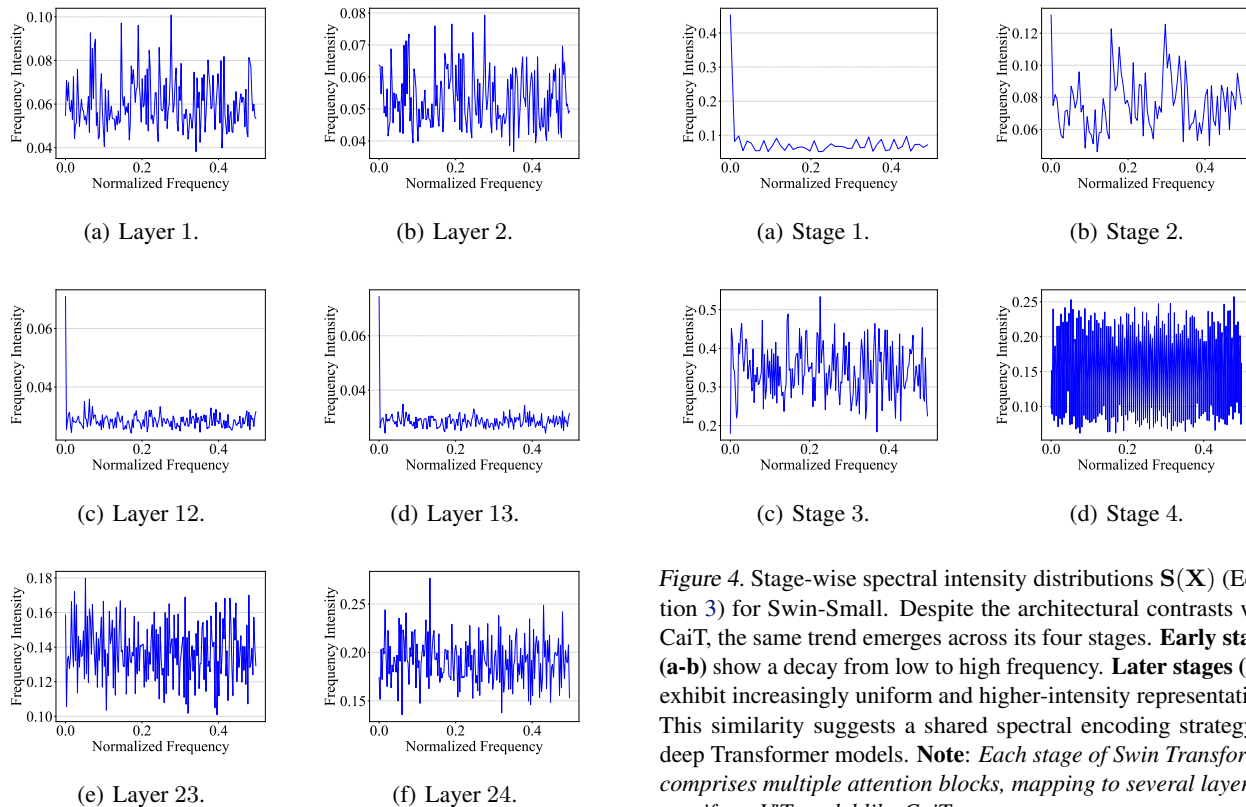


Figure 3. Layer-wise spectral intensity distributions $\mathbf{S}(\mathbf{X})$ (Equation 3) for representative layers of CaiT-S24. The visualization reveals distinct encoding patterns across network depths. **Early layers (a-b)** exhibit approximately uniform intensities across frequencies. **Middle layers (c-d)** show a marked decay from low to high frequency. **Final layers (e-f)** once again become relatively uniform but at distinctly higher overall intensities.

component. Hence, $\mathbf{S}(\mathbf{X})$ offers a *layer-wise* view into the encoding patterns of neural networks in the spectral domain.

To quantify the overall frequency intensity of a single layer, we further average $\mathbf{S}(\mathbf{X})$ over the channel dimension:

$$\ell(\mathbf{X}) = \frac{1}{C} \sum_{c=1}^C \mathbf{S}(\mathbf{X}). \quad (4)$$

The scalar $\ell(\mathbf{X})$ thus captures the aggregate spectral intensity of feature map of a single layer or stage in the model. Higher $\ell(\mathbf{X})$ values typically indicate layers encoding more complex or diverse features, making them strong candidates for transfer in KD.

Finally, by computing $\ell(\mathbf{X})$ across multiple layers or stages, we obtain

$$L(\mathbf{X}) = \{\ell^{(1)}(\mathbf{X}), \ell^{(2)}(\mathbf{X}), \dots, \ell^{(n)}(\mathbf{X})\}, \quad (5)$$

where n denotes the total number of layers or stages under

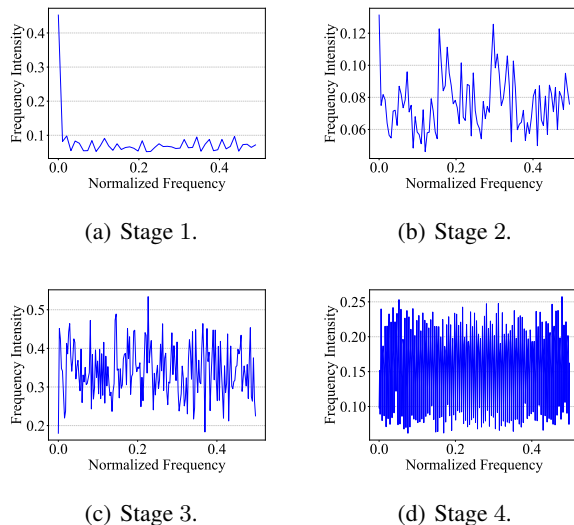


Figure 4. Stage-wise spectral intensity distributions $\mathbf{S}(\mathbf{X})$ (Equation 3) for Swin-Small. Despite the architectural contrasts with CaiT, the same trend emerges across its four stages. **Early stages (a-b)** show a decay from low to high frequency. **Later stages (c-d)** exhibit increasingly uniform and higher-intensity representations. This similarity suggests a shared spectral encoding strategy in deep Transformer models. **Note:** Each stage of Swin Transformer comprises multiple attention blocks, mapping to several layers in a uniform ViT model like CaiT.

consideration. The collection $L(\mathbf{X})$ provides a *model-wise* perspective on how information complexity evolves with network depth.

In summary, our spectral analysis provides both *model-wise* and *layer-wise* insights into the flow of information in models. This dual perspective provides new analytical tools for machine learning models.

2.2. Analysis of ViTs

In this section, we show how ViTs can be analyzed through SpectralKD, and then optimize KD.

2.2.1. MODEL-WISE ANALYSIS

To investigate how information flows through ViTs, SpectralKD framework is applied to CaiT-S24 (Touvron et al., 2021b), a model containing 24 Transformer layers. Figures 1(a) and 2 present two complementary visualizations of how frequency intensity evolves across layers, as computed by Equation 5.

The results in these figures highlight two main findings:

- U-Shaped Intensity Curve.** As seen in Figure 1(a), the average frequency intensities exhibit a U-shaped trend. The first and final few layers have substantially

higher intensities, suggesting that they encode more information-rich representations. Conversely, the middle layers demonstrate much lower intensity values, implying their role may focus more on feature extraction and transformation than on encoding new information.

2. **Skewed Distribution of Spectral Magnitude.** The histogram in Figure 2 confirms that only a few layers possess notably higher intensities, while the majority cluster around lower magnitude values. This skewed distribution suggests that certain peak layers could be especially beneficial in KD, as they appear to concentrate more complex or salient features.

2.2.2. LAYER-WISE ANALYSIS

We next investigate the *layer-wise* spectral distribution (computed according to Equation 3) within individual feature maps at various network depths. Figure 3 presents the frequency distributions of six representative layers in CaiT-S24, revealing three main patterns:

1. **Early layers (e.g., Figure 3(a), 3(b)).** These layers show relatively uniform intensity distributions across the frequency bands but maintain moderate overall intensities. This suggests that fine-grained (high-frequency) information is preserved early on, likely to capture detailed features from the input.
2. **Middle layers (e.g., Figure 3(c), 3(d), layers 12-13).** In contrast to the early layers, the middle layers show a pronounced decay from low to high frequencies. This pattern implies that the network at this depth transforms the features into more abstract and smoother representations. Such an observation may yield new insights into how ViTs achieve strong generalization.
3. **Final layers (e.g., Figure 3(e), 3(f)).** In the last few layers, the spectral distributions revert to a more uniform distribution but with significantly higher intensities. This pattern indicates a strong utilization of the channel dimension to encode both high- and low-frequency information, which is beneficial for fine-grained classification.

A complete visualization of spectral distributions across all layers of CaiT is available in Appendix A.

2.2.3. CROSS-ARCHITECTURE ANALYSIS

To broaden our analysis, we further study the Swin-Small (Liu et al., 2021) model, which adopts a hierarchical design quite distinct from CaiT. Each stage of Swin Transformer comprises multiple attention blocks, mapping to several layers in a uniform model like CaiT. Thus, the first stage

of Swin Transformer may contain enough attention blocks parallel to middle layers of CaiT.

As shown in Figure 4, the frequency distributions across its four stages display a surprisingly similar pattern to CaiT, highlighting a convergent encoding strategy of both architectures. Similar to the middle layers of CaiT, the early stages of Swin Transformer show a decay from low to high frequency. The later stage exhibits an almost uniform distribution in spectral domain at relatively high magnitudes, which is also similar to the final layers of CaiT.

Interestingly, patterns in both later stages and final layers differ from typical natural signals (where intensity tends to decay at higher frequencies). This suggests that deep networks develop their own artificial signal characteristics, actively encoding final representations based on abstract features in the middle layers or early stages rather than merely preserving natural image statistics.

2.2.4. IMPLICATIONS FOR KD

A deeper understanding of both the *model-wise* flow of information and the *layer-wise* encoding patterns in ViTs is essential for designing an effective knowledge transfer strategy in KD. When performing feature-based knowledge distillation, two fundamental challenges arise: (1) identifying the best layers for distillation from an architectural perspective, and (2) aligning the features across the channel dimension within intermediate layer representations. Although hierarchical architectures such as the Swin Transformer naturally suggest distillation points at the boundaries of their stages, selecting appropriate distillation layers in uniform architectures (such as ViT (Dosovitskiy, 2020), CaiT (Touvron et al., 2021b), and DeiT (Touvron et al., 2021a)), which comprise sequences of nearly identical Transformer blocks, remains an open question.

In conventional signal processing (Gonzales & Wintz, 1987), spectral intensity does not inherently correlate with information richness. However, through above *model-wise* and *layer-wise* analyses of ViTs, we observe a critical phenomenon: layers with higher aggregate spectral intensities $\ell(\mathbf{X})$ consistently demonstrate more uniform frequency energy distributions. This suggests that such layers encode diverse features spanning both low-frequency global patterns and high-frequency local details. We hypothesize this phenomenon may be attributed to ViT-specific regularization mechanisms, such as Layer Normalization, which suppress frequency-specific biases and promote balanced utilization of multi-band spectral features.

Our empirical findings in ViTs reveal a strong correlation between high spectral intensity and multi-frequency encoding capability. To balance computational efficiency with interpretability, we adopt spectral intensity as a practical

proxy for information richness in this work. This choice provides a principled criterion for identifying critical distillation layers, enabling efficient and effective knowledge transfer. Our spectral analysis leads to several practical guidelines for feature-based KD:

- In uniform Transformer architectures like CaiT, both early and final few layers exhibit the higher spectral intensities. These layers are thus prime distillation points for transferring knowledge most effectively.
- Since early and final few layers display strong utilization of all frequency bands, effective KD should aim to help the student model inherit this multi-frequency encoding capability. Aligned feature channels can thus facilitate richer representations.

In the next section, we will build a simple distillation strategy based on the above practical guidelines, and then in the Section 4, we present empirical evaluations that confirm these conclusions.

3. Frequency Alignment for KD

Motivated by the above insights, we introduce a frequency alignment distillation method that explicitly aligns the spectral characteristics of student and teacher networks.

3.1. Method Overview

Let $\mathbf{F}_s \in \mathbb{R}^{B \times C_s \times H \times W}$ and $\mathbf{F}_t \in \mathbb{R}^{B \times C_t \times H \times W}$ denote the intermediate feature maps of student and teacher models from particular layer or stage, respectively, where B is the batch size, C_s and C_t denote the number of channels, and H, W represent the spatial dimensions.

Our approach first aligns the channel dimensions of these feature maps and then performs a 2D FFT over their spatial dimensions¹ before computing the distillation loss. By applying a 2D Fourier transform to their feature maps, we capture and align both low-frequency (global) and high-frequency (fine-grained) details, thus enabling richer knowledge transfer.

3.2. Alignment Strategy

Channel Dimension Alignment. To adapt different channel numbers between student and teacher, we apply 3D adaptive average pooling:

$$\mathbf{F}_s = \text{AdaptiveAvgPool}(\mathbf{F}_s) \quad \text{if } C_s > C_t, \quad (6)$$

$$\mathbf{F}_t = \text{AdaptiveAvgPool}(\mathbf{F}_t) \quad \text{if } C_s < C_t. \quad (7)$$

¹In earlier spectral analysis (Section 2), we use 1D FFT across channels to characterize frequency intensities. Here, we use 2D FFT across spatial dimensions to align global and local features, which is more natural for data like images.

After this operation, both feature maps are in the shape of $\mathbb{R}^{B \times C \times H \times W}$, where $C = \min(C_s, C_t)$. We choose adaptive average pooling over linear projections or additional attention layers for two reasons: (1) it preserves the spatial structure of features while adjusting channel dimension, and (2) it remains simple enough to allow clear interpretability of the distillation process. This design follows our earlier analysis (Section 2.2), which finds that Transformer networks tend to leverage all channels for information encoding.

Fast Fourier Transform. We then apply the 2D real-valued Fast Fourier Transform (RFFT2) along the spatial dimensions of each channel in the aligned feature maps:

$$\mathcal{F}(\mathbf{F}_s) = \text{RFFT2}(\mathbf{F}_s), \quad (8)$$

$$\mathcal{F}(\mathbf{F}_t) = \text{RFFT2}(\mathbf{F}_t). \quad (9)$$

To simplify computation and loss definition, we separate the real and imaginary parts and then stack them along a new dimension:

$$\mathcal{F}_{\text{real}}(\mathbf{F}_s) = \text{Re}(\mathcal{F}(\mathbf{F}_s)), \quad (10)$$

$$\mathcal{F}_{\text{imag}}(\mathbf{F}_s) = \text{Im}(\mathcal{F}(\mathbf{F}_s)), \quad (11)$$

$$\mathcal{F}_{\text{stack}}(\mathbf{F}_s) = \text{Stack}(\mathcal{F}_{\text{real}}(\mathbf{F}_s), \mathcal{F}_{\text{imag}}(\mathbf{F}_s)). \quad (12)$$

The same operations are applied to the feature maps of teacher.

3.3. Loss Function

Frequency Alignment Loss. We use the Mean Squared Error (MSE) loss to measure the difference between the student and teacher representations in the frequency domain:

$$\mathcal{L}_{\text{FFT}} = \text{MSE}(\mathcal{F}_{\text{stack}}(\mathbf{F}_s) - \mathcal{F}_{\text{stack}}(\mathbf{F}_t)). \quad (13)$$

This penalizes discrepancies across both low- and high-frequency components, ensuring that the student learns to capture global structure (low frequency) as well as fine details (high frequency).

Training Objective. To harness both conventional KD loss and our proposed frequency alignment, we combine \mathcal{L}_{FFT} with the standard KD loss (Hinton, 2015):

$$\mathcal{L}_{\text{KD}} = (1 - \alpha)\mathcal{L}_{\text{CE}}(f_s(\mathbf{x}), y) + \alpha T^2 \mathcal{L}_{\text{KL}}\left(\frac{f_s(\mathbf{x})}{T}, \frac{f_t(\mathbf{x})}{T}\right), \quad (14)$$

where \mathcal{L}_{CE} is the cross-entropy loss between the student predictions $f_s(\mathbf{x})$ and ground-truth labels y , and \mathcal{L}_{KL} is the Kullback-Leibler divergence. The temperature T smooths the logits of teacher, and α balances the two terms.

We then form the total loss:

$$\mathcal{L}_{\text{Total}} = \mathcal{L}_{\text{KD}} + \beta \mathcal{L}_{\text{FFT}}, \quad (15)$$

where β controls how heavily the frequency alignment term influences training. This objective encourages the student to learn both decision boundaries (through standard KD) and internal frequency representations (through \mathcal{L}_{FFT}), ultimately yielding a more robust and comprehensive knowledge transfer.

4. Experiments

We demonstrate the effectiveness of SpectralKD through extensive experiments on image classification task. Our results show that our SpectralKD leads to SOTA performance. This section details our experimental setup, presents comprehensive results, and validates our approach through ablation studies.

4.1. Experimental Setup

Dataset and Models. We conduct experiments on the ImageNet-1k dataset (Deng et al., 2009), which comprises 1.28M training images and 50K validation images across 1,000 classes. We use multiple vision transformer architectures for our evaluations.

Implementation Details. All experiments are conducted on 2 NVIDIA RTX 4090D GPUs with a batch size of 256. Training DeiT-Tiny requires approximately 184 GPU hours. Our implementation is in PyTorch, and we build upon the *timm* library (Wightman, 2019) for model architectures and pretrained weights.

Student Networks. We evaluate several vision transformer variants as student models, all trained exclusively on ImageNet-1k: (1) DeiT-Tiny and DeiT-Small, both trained from scratch following the DeiT settings (Touvron et al., 2021a), and (2) Swin-Tiny, also trained from scratch based on the original Swin Transformer settings (Liu et al., 2021).

Teacher Networks. We employ CaiT and Swin-Small architectures as teacher models, both pretrained solely on ImageNet-1k (i.e., without ImageNet-22k pretraining). We obtain the teacher checkpoints from the *timm* library.

Hyperparameters. Unless otherwise stated, we use a distillation temperature of 1, $\alpha = 0.9$, and $\beta = 0.2$ for DeiT experiments, while $\beta = 0.05$ is used for Swin Transformer experiments.

4.2. Results and Analysis

Table 1 compares our SpectralKD derived method with SOTA KD approaches on ImageNet-1k, using CaiT-S24 (47M parameters) as the teacher. Guided by our *model-wise* and *layer-wise* spectral analysis insights of ViTs (Section 2.2), we apply distillation to the first two and final six layers of both teacher and student. We train DeiT-Tiny for 400 epochs and DeiT-Small for 500 epochs under the DeiT

training protocol (Touvron et al., 2021a), setting stochastic depth rate to 0.

DeiT-Tiny Results. With DeiT-Tiny (5M parameters) as the student model, SpectralKD achieves SOTA performance with a top-1 accuracy of 77.4%, an absolute improvement of 5.2% over the 72.2% baseline. It also outperforms the standard hard distillation baseline of 74.5%, demonstrating more efficient knowledge transfer.

DeiT-Small Results. For the larger DeiT-Small student (22M parameters), SpectralKD delivers similarly strong gains. It improves the baseline accuracy from 79.9% to 82.2%, outperforming the baseline by 2.3% and the hard distillation (81.3%) by 0.9% in absolute terms. The consistent performance across model scales underscores the effectiveness of our frequency-based distillation strategy for knowledge transfer.

Swin Transformer Results. We further evaluate SpectralKD on hierarchical transformer architectures. Using Swin-Small (50M parameters) as the teacher model and Swin-Tiny (29M parameters, 81.3% baseline) as the student model, SpectralKD achieves 82.7% top-1 accuracy (Table 2), improving on the baseline by 1.4%. This result indicates that SpectralKD effectively transfers knowledge across hierarchical transformer architectures with different attention mechanisms and feature hierarchies compared to DeiT models.

4.3. Ablation Study

To further validate the effectiveness of SpectralKD, we conduct ablation studies on ImageNet-1k with DeiT-Tiny as the student model.

Table 3 presents the results of different KD configurations. When combining SpectralKD with soft KD, the student model achieves the best performance with 77.4% top-1 accuracy, surpassing the baseline by 5.2%. The superior performance of the full model demonstrates that SpectralKD complements traditional knowledge distillation by capturing valuable spectral information not explicitly present in either hard or soft predictions.

Table 4 compares several layer matching strategies for CaiT-S24 (teacher) and DeiT-Tiny (student): uniform early-late layer matching, middle layer matching, and our proposed spectral-based layer matching. Aligning teacher layers $\mathcal{T} = \{1, 2, 19, 20, 21, 22, 23, 24\}$ with student layers $\mathcal{S} = \{1, 2, 7, 8, 9, 10, 11, 12\}$ via spectral analysis achieves the highest top-1 accuracy of 77.4%. This demonstrates that using non-uniform early and late few layers with high information intensity, as suggested by our SpectralKD framework, results in the most effective knowledge transfer.

Table 1. Classification accuracies on ImageNet-1K for DeiT-Tiny and DeiT-Small.

DISTILLATION METHOD	TEACHER	PARAMS	TOP-1 (%)	STUDENT	TOP-1 (%)
-	-	-	-	DEiT-TINY (5M)	72.2
HARD (TOUVRON ET AL., 2021A)	REGNETY-16GF	84M	82.9	DEiT-TINY (5M)	74.5
DEARKD (CHEN ET AL., 2022)	REGNETY-16GF	84M	82.9	DEiT-TINY (5M)	74.8
USKD (YANG ET AL., 2023)	REGNETY-16GF	84M	82.9	DEiT-TINY (5M)	75.0
SRD (MILES & MIKOLAJCZYK, 2024)	REGNETY-16GF	84M	82.9	DEiT-TINY (5M)	77.2
HARD (TOUVRON ET AL., 2021A)	CAiT-S24	47M	83.4	DEiT-TINY (5M)	74.5
MANIFOLD (HAO ET AL., 2022)	CAiT-S24	47M	83.4	DEiT-TINY (5M)	76.5
MASKEDKD (SON ET AL., 2025)	CAiT-S24	47M	83.4	DEiT-TINY (5M)	75.9
SPECTRALKD (OURS)	CAiT-S24	47M	83.4	DEiT-TINY (5M)	77.4
-	-	-	-	DEiT-SMALL (22M)	79.9
HARD (TOUVRON ET AL., 2021A)	REGNETY-16GF	84M	82.9	DEiT-SMALL (22M)	81.2
DEARKD (CHEN ET AL., 2022)	REGNETY-16GF	84M	82.9	DEiT-SMALL (22M)	81.5
USKD (YANG ET AL., 2023)	REGNETY-16GF	84M	82.9	DEiT-SMALL (22M)	80.8
SRD (MILES & MIKOLAJCZYK, 2024)	REGNETY-16GF	84M	82.9	DEiT-SMALL (22M)	82.1
HARD (TOUVRON ET AL., 2021A)	CAiT-S24	47M	83.4	DEiT-SMALL (22M)	81.3
MANIFOLD (HAO ET AL., 2022)	CAiT-S24	47M	83.4	DEiT-SMALL (22M)	82.2
SPECTRALKD (OURS)	CAiT-S24	47M	83.4	DEiT-SMALL (22M)	82.2

Table 2. Classification accuracies on ImageNet-1K for Swin-Tiny. ‡: Pretrained on ImageNet-22K.

DISTILLATION METHOD	TEACHER	PARAMS	TOP-1 (%)	STUDENT	TOP-1 (%)
-	-	-	-	SWIN-TINY (29M)	81.3
KD (HINTON, 2015)	SWIN-LARGE ‡	197M	86.3	SWIN-TINY (29M)	81.5
RKD (PARK ET AL., 2019)	SWIN-LARGE ‡	197M	86.3	SWIN-TINY (29M)	81.2
SRRL (YANG ET AL., 2021)	SWIN-LARGE ‡	197M	86.3	SWIN-TINY (29M)	81.5
DIST (HUANG ET AL., 2022)	SWIN-LARGE ‡	197M	86.3	SWIN-TINY (29M)	82.3
SCALEKD (FAN ET AL., 2024)	SWIN-LARGE ‡	197M	86.3	SWIN-TINY (29M)	83.8
MANIFOLD (HAO ET AL., 2022)	SWIN-SMALL	50M	83.2	SWIN-TINY (29M)	82.2
SPECTRALKD (OURS)	SWIN-SMALL	50M	83.2	SWIN-TINY (29M)	82.7

Table 3. Ablation study results on ImageNet-1K. DeiT-Tiny serves as the student model.

METHOD	TOP-1 (%)	Δ (%)
w/o KD	72.2	-
HARD KD	74.5	+2.3
SOFT KD	76.2	+4.0
SOFT KD + SPECTRALKD	77.4	+5.2

5. Distillation Dynamics

We analyze the dynamics of knowledge transfer between teacher and student models using our SpectralKD framework, providing insights into how the teacher’s information processing patterns influence the student’s learning trajectory. Specifically, we investigate how intermediate feature representations evolve during distillation and how these changes directly correlate with performance improvements.

Recall that the spectral intensity of each Transformer layer (Equation (5)) quantifies its information processing capacity. We compare three configurations: (1) the teacher model

(CAiT-S24, 83.4% top-1 accuracy), (2) the baseline student (DeiT-Tiny, 72.2% top-1 accuracy) trained without distillation, and (3) the distilled student (DeiT-Tiny) trained with SpectralKD (77.4% top-1 accuracy). Figure 1 illustrates the *model-wise* spectral intensity distributions across these configurations.

5.1. Teacher vs. Non-Distilled Student

As discussed in Section 2.2, the teacher model (Figure 1(a)) exhibits a distinct U-shaped spectral pattern, characterized by high intensity in early layers, a dip in the middle, and a resurgence in the final layers. In contrast, the baseline student (Figure 1(b)) shows a similar but attenuated trend. The early and late layers exhibit weaker spectral peaks, and the transition between middle and final layers is less defined. Fluctuations in the last few layers further suggest inefficiencies in feature encoding, where the student struggles to filter out redundant or noisy information.

These observations indicate that, without distillation, the baseline student fails to capture the teacher’s rich high-level features and lacks the capacity to suppress irrelevant signals,

Table 4. Layer matching strategies and corresponding performance on ImageNet-1K between CaiT-S24 (teacher) and DeiT-Tiny (student). †: Spectral analysis-based layer selection as described in Section 2.

MATCHING STRATEGY	TEACHER LAYERS \mathcal{T}	STUDENT LAYERS \mathcal{S}	TOP-1 (%)
EARLY-LATE	{1, 2, 3, 4, 21, 22, 23, 24}	{1, 2, 3, 4, 9, 10, 11, 12}	77.2
MIDDLE	{4, 5, 6, 7, 8, 9, 10, 11}	{10, 11, 12, 13, 14, 15, 16, 17}	77.0
SPECTRAL †	{1, 2, 19, 20, 21, 22, 23, 24}	{1, 2, 7, 8, 9, 10, 11, 12}	77.4

a critical capability inherited by the distilled student.

5.2. Impact of SpectralKD

When SpectralKD is applied to distill knowledge selectively from the teacher’s first two and last six layers, the student model (Figure 1(c)) shows a spectral profile closely aligned with the teacher. The early and late few layers exhibit sharper intensity increases, mirroring the teacher’s feature extraction and encoding patterns. Meanwhile, the middle layers display a streamlined intensity profile with reduced redundancy. This structural alignment likely contributes to the distilled student’s improved generalization, as evidenced by its +5.2% top-1 accuracy gain over the baseline.

Notably, this teacher-like spectral distribution emerges even though only a subset of student layers is explicitly aligned. The intermediate layers naturally adopt processing patterns resembling the teacher’s, demonstrating that selective distillation can induce global behavioral changes in the student.

5.3. Teacher as Implicit Feature Refiner

Our findings suggest that the teacher acts as an *implicit feature refiner* during distillation: by transferring noise-tolerant representations, it guides the student to prioritize discriminative patterns. For instance, the middle layers of the distilled student learn smoother, more abstract features compared to the baseline, even though these layers are not directly distilled. This phenomenon is similar to the finding in Section 2.2 that the teacher’s middle layers can filter out high-frequency information and encode abstract features.

This insight extends the utility of KD beyond mere model compression. A teacher with robust representational capacity can refine the student’s feature learning process, imparting resistance to noise and improving discriminative power.

In summary, our empirical analysis demonstrates that effective knowledge distillation transcends output distribution matching. It necessitates aligning the student’s internal spectral patterns with the teacher’s, thereby replicating the hierarchical information flow critical for robust performance. This principle not only explains the efficacy of SpectralKD but also opens avenues for designing distillation strategies grounded in interpretable distillation dynamics.

6. Conclusion

In this paper, we introduce SpectralKD, a unified framework for interpreting and distilling ViTs via spectral analysis. Our key contributions stem from both theoretical insights and practical advancements. Our analyses reveal two key findings about ViTs: (1) in uniform transformer architectures, only a few early and late layers exhibit particularly high spectral intensities (Section 2.2.1), guiding us toward optimal points for KD, and (2) despite their different designs, hierarchical transformers (e.g., Swin) and uniform transformers (e.g., CaiT) share remarkably similar layer-wise encoding patterns (Section 2.2.2 and 2.2.3), deriving alignment guidelines for KD.

Building on these observations, we propose a simple, parameter-free KD strategy (Section 3), achieving SOTA performance on ImageNet-1K. Post-training analysis (Section 5) demonstrates that the distilled student mirrors the teacher’s spectral patterns and hierarchical information flow, underscoring the framework’s ability to transfer both local and global knowledge.

These results advance our understanding of how and why KD works for ViTs, opening a new research area we term “distillation dynamics”. By bridging interpretability and practical distillation, SpectralKD provides an analytical tool for future work in model compression, transfer learning, and transparent deep learning.

Impact Statement

Looking forward, our work opens several promising directions for future research. The spectral analysis framework could be extended to other network architectures and tasks beyond vision transformers. The observed relationship between spectral patterns and model performance suggests potential applications in neural architecture search and automated model compression. Additionally, our findings about information flow in transformers may inform the design of more efficient architectures that maintain high performance with reduced computational requirements.

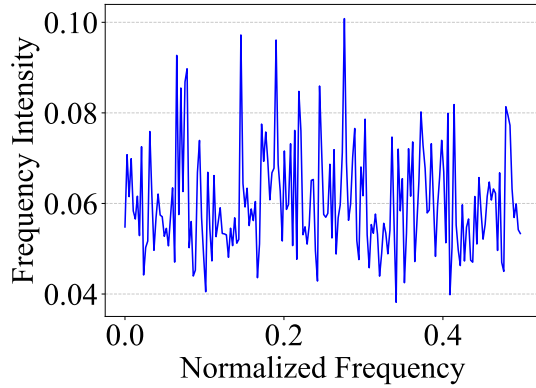
The broader impact of this work extends beyond knowledge distillation. Our spectral analysis framework provides a new lens for understanding deep neural networks, potentially influencing how we approach model design, optimization,

and analysis. We believe these insights will contribute to the development of more efficient and interpretable deep learning systems.

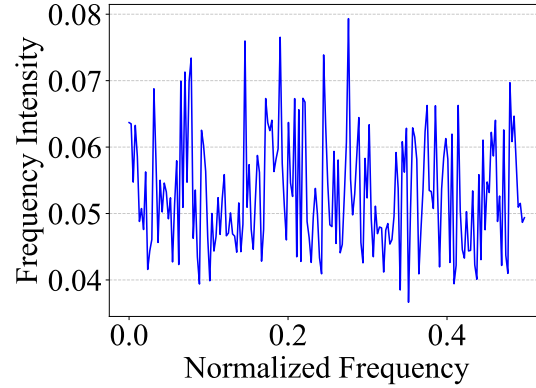
References

- Abnar, S. and Zuidema, W. Quantifying attention flow in transformers. *arXiv preprint arXiv:2005.00928*, 2020.
- Allen-Zhu, Z. and Li, Y. Towards understanding ensemble, knowledge distillation and self-distillation in deep learning, 2023.
- Bar-Shalom, G., Bevilacqua, B., and Maron, H. Subgraphormer: Unifying subgraph GNNs and graph transformers via graph products. In *Forty-first International Conference on Machine Learning*, 2024.
- Brown, T., Mann, B., Ryder, N., Subbiah, M., Kaplan, J., Dhariwal, P., Neelakantan, A., Shyam, P., Sastry, G., Askell, A., et al. Language models are few-shot learners. *Advances in Neural Information Processing Systems*, 33: 1877–1901, 2020.
- Caron, M., Touvron, H., Misra, I., Jégou, H., Mairal, J., Bojanowski, P., and Joulin, A. Emerging properties in self-supervised vision transformers. In *Proceedings of the IEEE/CVF international conference on computer vision*, pp. 9650–9660, 2021.
- Chandrasegaran, K., Tran, N.-T., Zhao, Y., and Cheung, N.-M. Revisiting label smoothing and knowledge distillation compatibility: What was missing? In *International Conference on Machine Learning*, pp. 2890–2916. PMLR, 2022.
- Chefer, H., Gur, S., and Wolf, L. Transformer interpretability beyond attention visualization. In *Proceedings of the IEEE/CVF conference on computer vision and pattern recognition*, pp. 782–791, 2021.
- Chen, X., Cao, Q., Zhong, Y., Zhang, J., Gao, S., and Tao, D. Dearkd: data-efficient early knowledge distillation for vision transformers. In *Proceedings of the IEEE/CVF conference on computer vision and pattern recognition*, pp. 12052–12062, 2022.
- Choudhary, T., Mishra, V., Goswami, A., and Sarangapani, J. A comprehensive survey on model compression and acceleration. *Artificial Intelligence Review*, 53:5113–5155, 2020.
- Deng, J., Dong, W., Socher, R., Li, L.-J., Li, K., and Fei-Fei, L. Imagenet: A large-scale hierarchical image database. In *2009 IEEE conference on computer vision and pattern recognition*, pp. 248–255. Ieee, 2009.
- Devlin, J. Bert: Pre-training of deep bidirectional transformers for language understanding. *arXiv preprint arXiv:1810.04805*, 2018.
- Dosovitskiy, A. An image is worth 16x16 words: Transformers for image recognition at scale. *arXiv preprint arXiv:2010.11929*, 2020.
- Fan, J., Li, C., Liu, X., and Yao, A. Scalekd: Strong vision transformers could be excellent teachers. *arXiv preprint arXiv:2411.06786*, 2024.
- Gonzales, R. C. and Wintz, P. *Digital image processing*. Addison-Wesley Longman Publishing Co., Inc., 1987.
- Han, K., Xiao, A., Wu, E., Guo, J., Xu, C., and Wang, Y. Transformer in transformer. *Advances in neural information processing systems*, 34:15908–15919, 2021.
- Han, K., Wang, Y., Chen, H., Chen, X., Guo, J., Liu, Z., Tang, Y., Xiao, A., Xu, C., Xu, Y., et al. A survey on vision transformer. *IEEE transactions on pattern analysis and machine intelligence*, 45(1):87–110, 2022.
- Hao, Z., Guo, J., Jia, D., Han, K., Tang, Y., Zhang, C., Hu, H., and Wang, Y. Learning efficient vision transformers via fine-grained manifold distillation. *Advances in Neural Information Processing Systems*, 35:9164–9175, 2022.
- Hinton, G. Distilling the knowledge in a neural network. *arXiv preprint arXiv:1503.02531*, 2015.
- Huang, T., You, S., Wang, F., Qian, C., and Xu, C. Knowledge distillation from a stronger teacher. *Advances in Neural Information Processing Systems*, 35:33716–33727, 2022.
- Li, X., Ding, H., Yuan, H., Zhang, W., Pang, J., Cheng, G., Chen, K., Liu, Z., and Loy, C. C. Transformer-based visual segmentation: A survey. *IEEE Transactions on Pattern Analysis and Machine Intelligence*, 2024.
- Liu, Z., Lin, Y., Cao, Y., Hu, H., Wei, Y., Zhang, Z., Lin, S., and Guo, B. Swin transformer: Hierarchical vision transformer using shifted windows. In *Proceedings of the IEEE/CVF international conference on computer vision*, pp. 10012–10022, 2021.
- Menon, A. K., Rawat, A. S., Reddi, S., Kim, S., and Kumar, S. A statistical perspective on distillation. In *International Conference on Machine Learning*, pp. 7632–7642. PMLR, 2021.
- Miles, R. and Mikolajczyk, K. Understanding the role of the projector in knowledge distillation. In *Proceedings of the AAAI Conference on Artificial Intelligence*, volume 38, pp. 4233–4241, 2024.

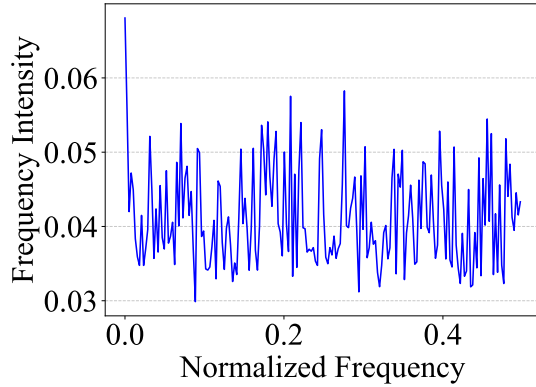
- Pan, B., Panda, R., Jiang, Y., Wang, Z., Feris, R., and Oliva, A. Ia-red²: Interpretability-aware redundancy reduction for vision transformers, 2021.
- Park, W., Kim, D., Lu, Y., and Cho, M. Relational knowledge distillation. In *Proceedings of the IEEE/CVF conference on computer vision and pattern recognition*, pp. 3967–3976, 2019.
- Pham, C., Nguyen, V.-A., Le, T., Phung, D., Carneiro, G., and Do, T.-T. Frequency attention for knowledge distillation. In *Proceedings of the IEEE/CVF Winter Conference on Applications of Computer Vision*, pp. 2277–2286, 2024.
- Phuong, M. and Lampert, C. Towards understanding knowledge distillation. In *International conference on machine learning*, pp. 5142–5151. PMLR, 2019.
- Raghu, M., Unterthiner, T., Kornblith, S., Zhang, C., and Dosovitskiy, A. Do vision transformers see like convolutional neural networks? *Advances in neural information processing systems*, 34:12116–12128, 2021.
- Rao, Z., Guo, J., Lu, X., Liang, J., Zhang, J., Wang, H., Wei, K., and Cao, X. Dual expert distillation network for generalized zero-shot learning. *arXiv preprint arXiv:2404.16348*, 2024.
- Son, S., Ryu, J., Lee, N., and Lee, J. The role of masking for efficient supervised knowledge distillation of vision transformers. In *European Conference on Computer Vision*, pp. 379–396. Springer, 2025.
- Touvron, H., Cord, M., Douze, M., Massa, F., Sablayrolles, A., and Jégou, H. Training data-efficient image transformers & distillation through attention. In *International conference on machine learning*, pp. 10347–10357. PMLR, 2021a.
- Touvron, H., Cord, M., Sablayrolles, A., Synnaeve, G., and Jégou, H. Going deeper with image transformers. In *Proceedings of the IEEE/CVF international conference on computer vision*, pp. 32–42, 2021b.
- Vaswani, A. Attention is all you need. *Advances in Neural Information Processing Systems*, 2017.
- Wightman, R. Pytorch image models. <https://github.com/rwightman/pytorch-image-models>, 2019.
- Xu, B., Zhou, Y., and Bian, X. Self-supervised learning based on transformer for flow reconstruction and prediction. *Physics of Fluids*, 36(2), 2024.
- Yang, J., Martinez, B., Bulat, A., Tzimiropoulos, G., et al. Knowledge distillation via softmax regression representation learning. *International Conference on Learning Representations (ICLR)*, 2021.
- Yang, Z., Zeng, A., Li, Z., Zhang, T., Yuan, C., and Li, Y. From knowledge distillation to self-knowledge distillation: A unified approach with normalized loss and customized soft labels. In *Proceedings of the IEEE/CVF International Conference on Computer Vision*, pp. 17185–17194, 2023.
- Yeh, C., Chen, Y., Wu, A., Chen, C., Viégas, F., and Wattenberg, M. Attentionviz: A global view of transformer attention. *IEEE Transactions on Visualization and Computer Graphics*, 2023.
- Yu, L. and Xiang, W. X-pruner: explainable pruning for vision transformers. In *Proceedings of the IEEE/CVF Conference on Computer Vision and Pattern Recognition (CVPR)*, pp. 24355–24363, June 2023.
- Zeng, J., Yang, Z., Yang, Q., Yang, L., and Lin, H. Peeling back the layers: Interpreting the storytelling of vit. In *Proceedings of the 32nd ACM International Conference on Multimedia*, pp. 7298–7306, 2024.
- Zimmermann, R. S., Klein, T., and Brendel, W. Scale alone does not improve mechanistic interpretability in vision models. *Advances in Neural Information Processing Systems*, 36, 2024.

A. Complete Spectral Distribution Analysis Across All Layers of CaiT

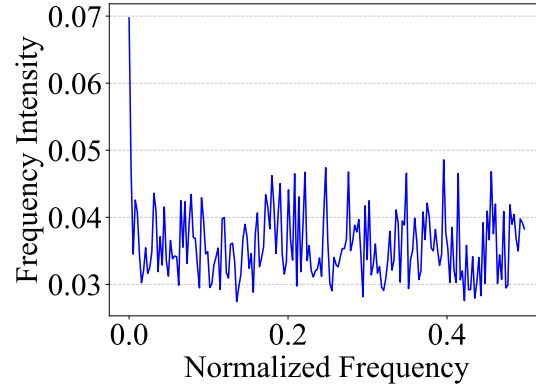
(a) Layer 1.



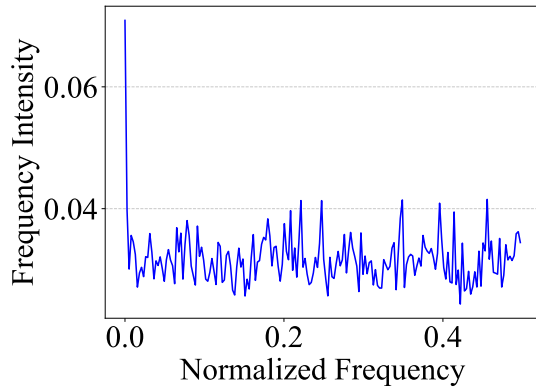
(b) Layer 2.



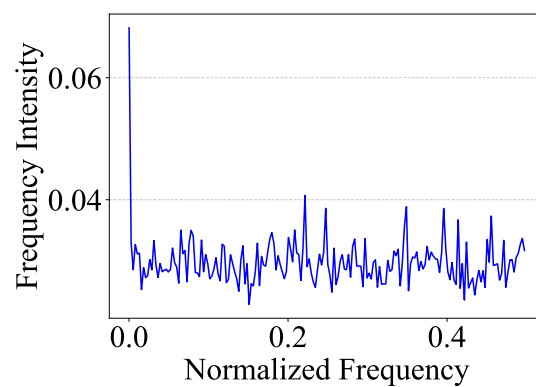
(c) Layer 3.



(d) Layer 4.

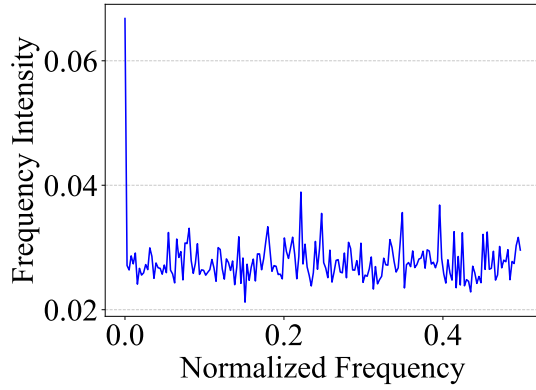


(e) Layer 5.

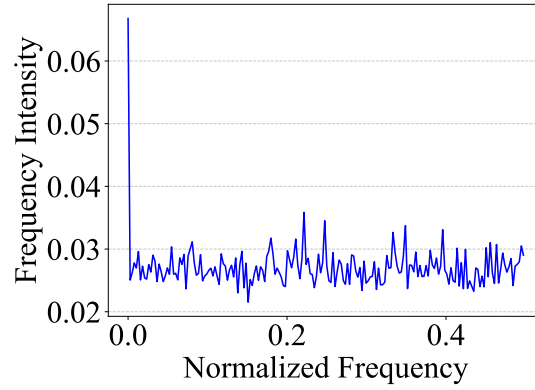


(f) Layer 6.

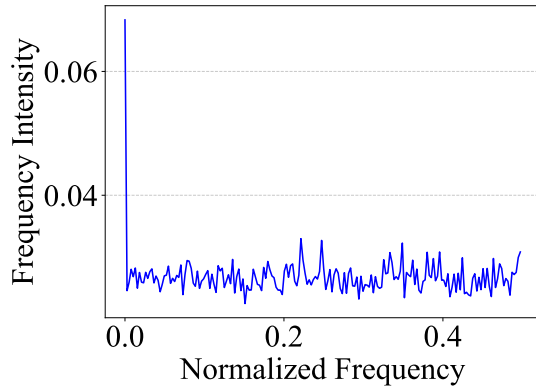
Figure 5. Spectral intensity distributions $S(\mathbf{X})$ computed using Equation (3) for layers (1-6) of CaiT-S24 feature maps.



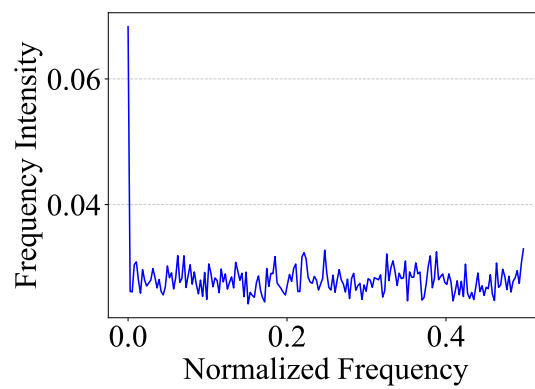
(a) Layer 7.



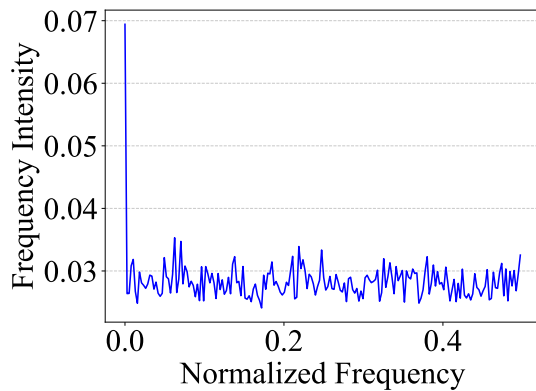
(b) Layer 8.



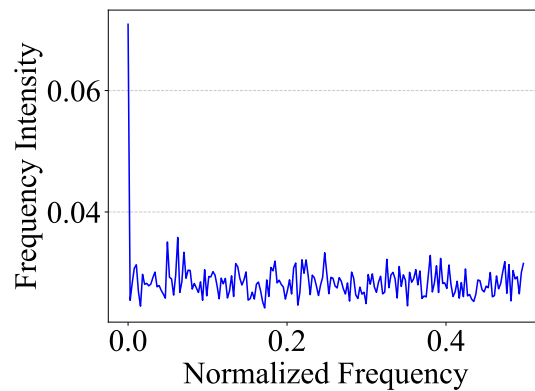
(c) Layer 9.



(d) Layer 10.



(e) Layer 11.



(f) Layer 12.

Figure 6. Spectral intensity distributions $\mathbf{S}(\mathbf{X})$ computed using Equation (3) for layers (7-12) of CaiT-S24 feature maps.

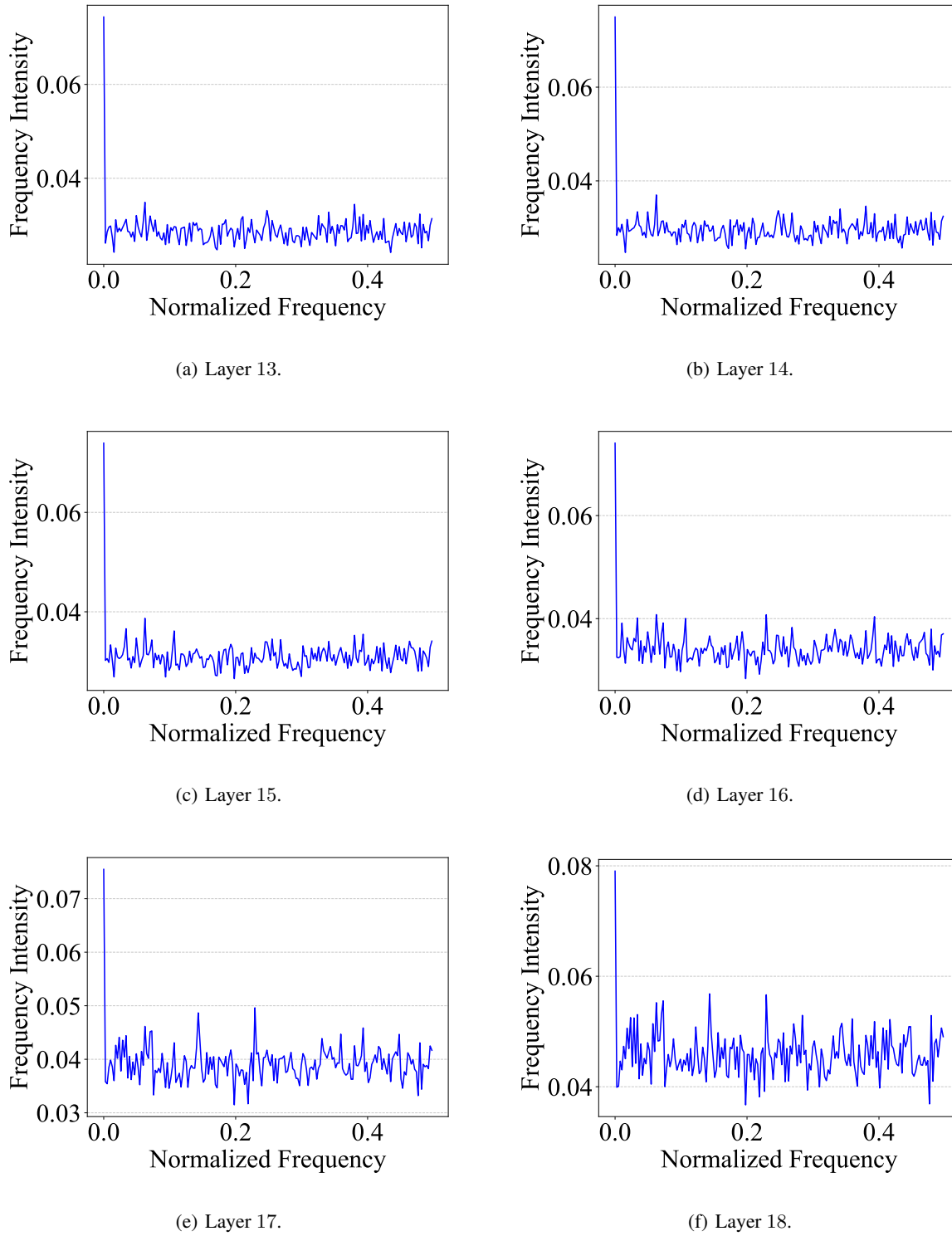
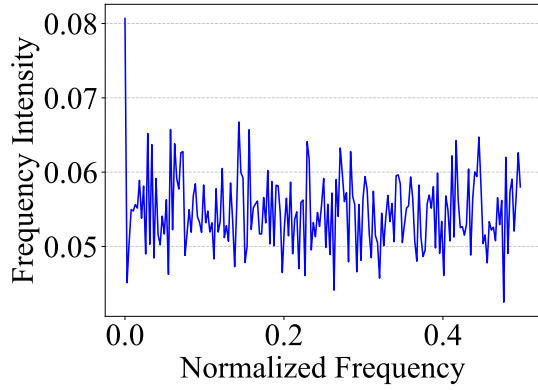
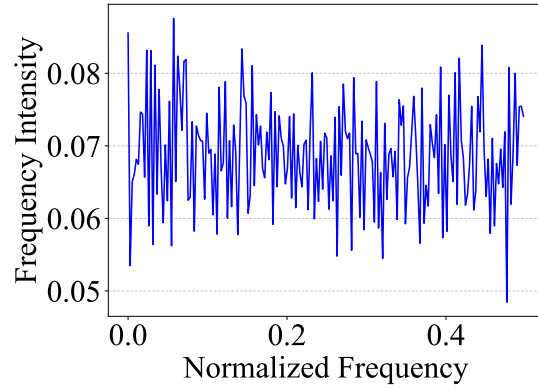


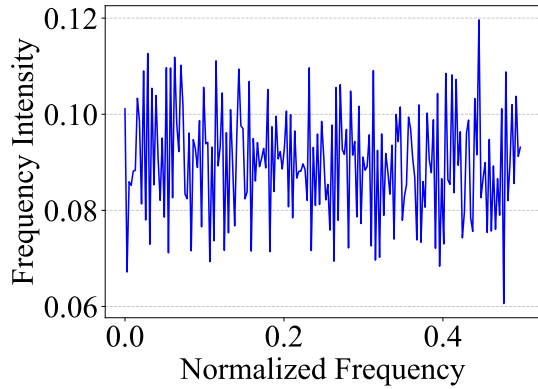
Figure 7. Spectral intensity distributions $S(\mathbf{X})$ computed using Equation (3) for layers (13-18) of CaiT-S24 feature maps.



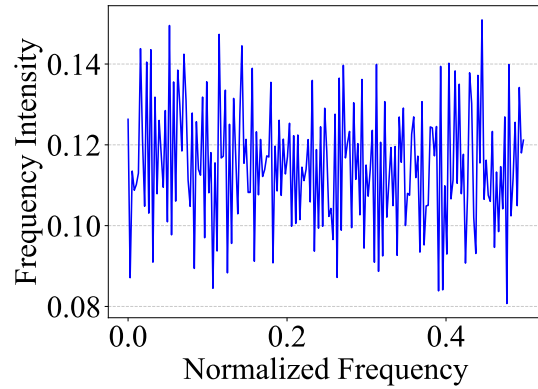
(a) Layer 19.



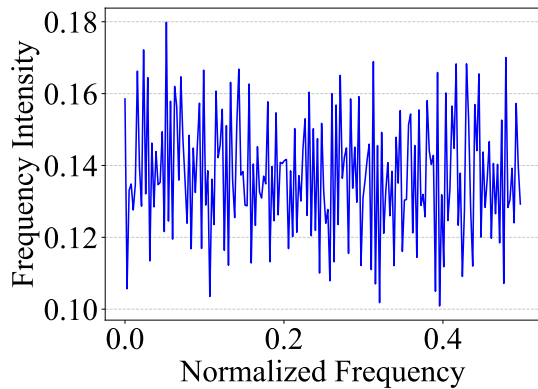
(b) Layer 20.



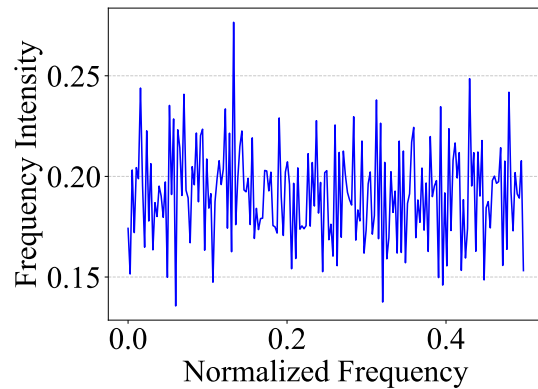
(c) Layer 21.



(d) Layer 22.



(e) Layer 23.



(f) Layer 24.

Figure 8. Spectral intensity distributions $S(\mathbf{X})$ computed using Equation (3) for layers (19-24) of CaiT-S24 feature maps.